JOURNAL OF ENGINEERING RESEARCH AND APPLIED SCIENCES (JERAS)
9th Edition – September 2021, (Hoon – Libya), **ISSN 2414-6515**

Numerical Study of Eccentrically Loaded Strip Footing Resting on Reinforced Sand by Using PLAXIS 2D Software

Aziza M. M. Elgerari azizaelgerari@yahoo.com
Ayad A.Mohammed aermila@yahoo.com
Salem M. Ali Salem_Eshtiwy_84@yahoo.com
Civil Engineering Department, Faculty of Engineering, Sirte University, Sirte, Libya

Abstract

The present paper aims to evaluate the performance of bearing capacity of eccentrically loaded strip footing supporting on unsymmetrical geogrid reinforced sand. More specifically to study the behavior of such eccentrically loaded strip footing supported on sand at different relative densities (dense, medium, and loose) reinforced with nonsymmetrical geosynthetic layers. A numerical study of the behavior of an eccentrically loaded strip footing resting on symmetrical and unsymmetrical geosynthetic reinforced sand is done. Particular attention was given to simulate strip footing constructed on unsymmetrical geogrid layers with eccentricity in one direction of the strip footing. Several configurations of geogrid layers such as different number (N), length (L), geogrid layer eccentricity (e_G) along with the effect of the sand relative density (R_d), the average unit weight (γ), and the load eccentricity (e_L) were investigated. The numerical study on a plane strain prototype strip footing was performed using finite element analysis PLAXIS 2D software. Tests results indicate that the strip footing performance could be appreciably improved by the inclusion of unsymmetrical geogrid layers leading to an economic design of the footing. However, the efficiency of the sand-geogrid system is dependent on the load eccentricity ratio (e_L/B) and several reinforcement parameters such as number of reinforcement layer (N), length of reinforcement (L), and eccentricity of reinforcement layer (e_G). The ultimate bearing capacity improvement due to the soil reinforcement and without reinforcement was represented using $q_{u(R)}$ and $q_{u(UR)}$ respectively. Therefore, it is useful to use the unsymmetrical layer of geogrid with eccentric load, and the appropriate value of geogrid eccentricity is (e_G=0.08B) that gives rate of improvement in the bearing capacity about 13.77% comparing to bearing capacity of the soil when laid the geogrid layers symmetrically beneath the strip footing, and, the percentage of improvement in the bearing capacity of the soil is up to 97.14% comparing to the soil bearing capacity without reinforcement. Also, the optimum length of reinforcement is equal five time of the footing width (L=5B), and the optimum number of reinforcement layers are four layers (N=4),

Keywords: Bearing capacity, Eccentric loads, Eccentric geogrid, Reinforced sand, Strip footing, Finite Element Method, PLAXIS 2D

1. PLAXIS 2D (V8.2) SOFTWARE DESCRIPTION

Shallow foundations such as a single footing are used in transmitting loads from the superstructure to the supporting soils. In many cases, these footings are frequently subjected to eccentric loading such as footings subjected to vertical load and bending moments due to lateral forces acting on structures from earth pressures, earthquakes, water, wind, etc. Sometimes, the footing eccentricity may be canceled. This could be achieved by constructing the footing with its center moved away from the center of the column a distance equal to the eccentricity value leading to uniform

pressure under the footing. However, this solution is not applicable in all the cases due to the interaction of the footing with the adjacent nearby footings making the design uneconomic and therefore, a structural problem arises. Due to eccentricity loading, the two edges of the footing settle by different amounts, causing the footing to tilt. The amount of the tilt and the pressure at the base depend upon the value of eccentricity to the footing width ratio. When this ratio is more than 1/6, the contact pressure will be tensile at the edge away from the load. However, as the soil cannot sustain tension, such a situation cannot develop. Hence, the contact area between the footing and the soil decreases with significant reduction in the bearing capacity and a great increase in footing size making the design uneconomical. Nasr and Azzam (2017).

PLAXIS 2D is a two-dimensional PLAXIS program is a finite element program for geotechnical applications and applications in foundation engineering in which models are used to simulate the soil behavior, developed for the analysis of foundation constructions including raft foundations and offshore structures. It is part of the PLAXIS product range, a suite of finite element program that are used worldwide for geotechnical engineering and design. Development of PLAXIS began in 1987 at the Technical University of Delft as an initiative of the Dutch department of Public Works and Water Management. The initial goal was to develop an easy-to-use 2D finite element code for the analysis of river embankments on the soft soils of the lowlands of Holland. In subsequent years, PLAXIS was extended to cover most other areas of geotechnical engineering. For each new 2D project to be analyzed it is important to create a geometry model first. A geometry model is a representation of a real two dimensional problem and is defined either by a plane strain or an ax isometric model. A geometry model should include a representative division of the subsoil into distinct soil layers, structural objects construction stage and loadings. The model must be sufficiently large so that the boundaries do not influence the results of the problem to be studied.

2. MODEL CONSTRUCTION DESCRIPTION

The nonlinear behavior of sand was modeled using the hardening soil model, which is an elastoplastic stress-strain model, formulated in the framework of friction hardening plasticity.

Plaxis program was carried out to study the behavior of an eccentrically loaded model strip footing resting on symmetrical and unsymmetrical geogrid reinforced sand. A series of two dimensional nonlinear FEA on a prototype plane strain footing on unreinforced and reinforced sand was performed to understand the deformation trends within the soil mass. A prototype strip footing was assumed to rest on a sandy soil and to extend laterally to a distance of four times and half of the footing width from each side and soil height in the model is 400cm.(The footing width B=75cm, and thickness of the footing t=20cm) as shown in figure.1. The parameters for footing are present in Table (2).

Initially, Series of tests on an eccentrically loaded model strip footing with different eccentricity (eL/B= 0, 0.05, 0.075, 0.1, 0.13 and 0.15) supported on both unreinforced sand and geogrid-reinforced loose, medium dense, and dense sands conditions were determined. Then series of tests were performed to study the effects of different geogrid parameters. The studied variables include the number of geogrid (N = 1, 2, 3, 4, 5), the length of the geogrid layers (L/B= 2, 3, 4, 5, 6), and hence the effect of the eccentricity of geogrid layer (eG/B= 0.42,

0.25, 0.1, 0.08, 0.07,and -0.08). It should be mentioned that the depth of a first geogrid layer is (u) and the vertical space between following layers is (h). The maximum improvement in bearing capacity of sand was obtained at the ratios of (u/B=0.33) and (h/B=0.53) as taken from previous reported research so these values were kept constant during the entire tests program ,Shin et al,(2002). The finite element program PLAXIS-2D (V8.2) centrically and eccentrically loaded the strip footing in both reinforced and unreinforced conditions, and the numerical model is presented in figure.2. that shows a geometry model consists of points, Lines, and clusters. Several parameters are crucial for the design of reinforced soil foundation (RSF). The purpose of these model tests was to examine the influences of the parameters those presented in table (1).

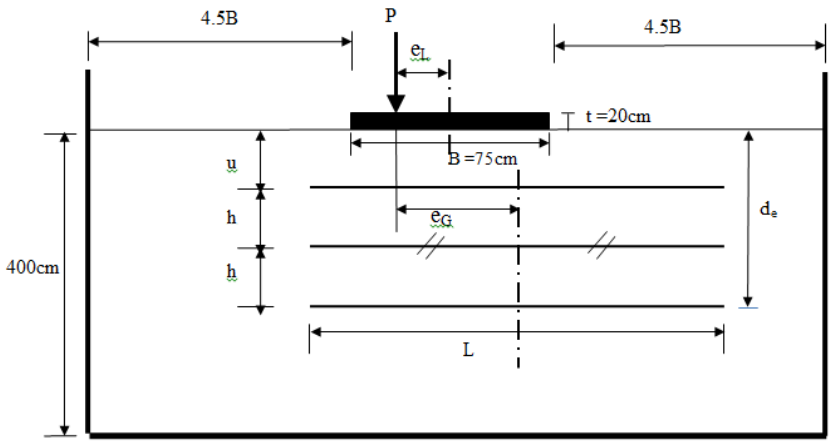

Fig. 1 Model of eccentrically loaded strip footing resting on geogrid-reinforced sand.

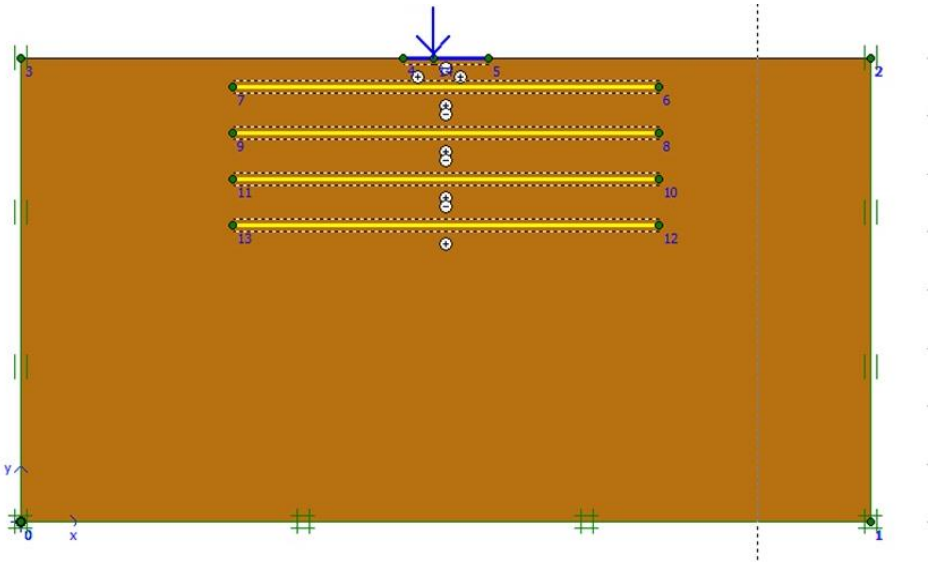

Fig..2 Model of eccentrically loaded strip footing created with PLAXIS 2D (V8.2).

Table 1 Details of models running parameters at PLAXIS-2D (V8.2) program

Group	Constant parameters	Variable parameters	Remarks
A	N=4,L/B=5, & Rd=80%	e_L/B=0, 0.05, 0.1, 0.13, 0.15,0.2	influence of eccentric load
	N=4,L/B=5, & Rd =55%	e_L /B =0, 0.05, 0.1, 0.13, 0.15,0.2	
	N=4, L/B=5, & Rd =35%	e_L /B =0, 0.05, 0.1, 0.13, 0.15,0.2	
	N=4, L/B=5, Rd =80% & e_L/B =0	e_G/B=0.42, 0.25, 0.1, 0.08, 0.07,-0.08	influence of eccentric geogrid
	N=4, L/B=5, Rd =80% & e_L /B=0.1	e_G /B=0.42, 0.25, 0.1, 0.08, 0.07,-0.08	
	N=4, L/B=5, Rd =80% & e_L /B=0.15	e_G /B=0.42, 0.25, 0.1, 0.08, 0.07,-0.08	
C	L/B=5, Rd =80% & e_L /B /B=0.1	N=1, 2, 3, 4& 5	influence of layer num-bers
	L/B=5, Rd =80% & e_L /B=0.15	N=1, 2, 3, 4& 5	
D	N=4, Rd =55% & e_L /B=0.15	L/B=2, 3, 4, 5&6	influence of geogrid lengths
	N=4, Rd =80% & e_L /B=0.15	L/B=2, 3, 4, 5&6	

Table 2. Material properties of the strip footing.

Parameter	Name	Value	Unit
Type of behavior	Material type	Elastic	-
Normal stiffness	EA	$3.6*10^6$	KN/m
Flexural rigidity	EI	$1.2*10^4$	KNm^2/m
Equivalent thickness	t	0.2	m
Poisson is ration	υ	1.2	-

2.1 Site Boundary Conditions

Its primary function is to impose a set of general boundary conditions to the geometry model. These boundary conditions are generated according to the following rules:

1. Vertical geometry lines for which the x-coordinate is equal to the lowest or highest x-coordinate in the model obtain a horizontal fixity (ux= 0)
2. .Horizontal geometry lines for which the y-coordinate is equal to the lowest y-coordinate in the model obtain a full fixity (ux = uy = 0)
3. Plates that extend to the boundary of the geometry model obtain a fixed rotation in the point at the boundary (φz = 0) if at least one of the displacement directions of that point is fixed. The boundary conditions in this modeling were chosen such that the vertical boundaries are free vertically and constrained horizontally while the bottom horizontal boundary is fully fixed.

Also, typical application of interfaces would be to create full interaction between structural objects (walls, plates, geogrids, etc.) and the surrounding soil model which is intermediate between smooth and fully rough. The roughness of the interaction is modeled by choosing a suitable value for the strength reduction factor in the interface (Rinter). This factor relates the interface strength (wall friction and adhesion) to the soil strength (friction angle and cohesion) this parameter is specified together with the soil strength parameters in a material data set for soil and interfaces .

Furthermore, the option of point load as external loading may be used to create point loads, which are actually line loads in the out-of-plane direction. The input values of point loads are given in force per unit of width (kN/m). The actual value that is applied in a calculation may be changed in the framework of staged construction. The footing load in this modeling was then applied in increasements accompanied by iterative analysis up to failure.

2.2Testing Materials Properties

Three different properties of sandy soil were used in the present study. The physical properties of soil are summarized in Table (3). However, the soil model in this analysis was the Moher-Coulomb. The basic feature of the hyperbolic model is the stress are dependency of soil stiffness. The limiting state of stress are described by means of the Secant Young's modulus(Eref50), Poission's ratio (υ), effective cohesion (c), angle of internal friction (φ), internal reduction factor (Rint), and the dilatancy angle ψ(equal φ -30). Since in PLAXIS program the quantity of zero for cohesion is not defined, a small value for cohesion was considered for sandy soil.

Table (3) Soil & geogrid properties used in the finite element analysis.

Parameter	Value	Value	Value	Value
Soil type	Dense sand	Medium sand	Loose sand	Geogrid
Material type	Drained	Drained	Drained	-
Material model	Mohr-coulomb	Mohr-coulomb	Mohr-coulomb	-
Soil unit weight(kN/m^3)	19.1	18.15	17.44	-
Residual angle of internal friction, ϕ	40°	35 °	31.5 °	-
Cohesion, c	0.0001	0.0001	0.0001	-
Dilatancy angle, ψ.	10	5	1.5	-
Modulus of elasticity, E (kN/m^2)	40000	30000	15000	-
				-
Poisson's ratio, ν	0.3	0.28	0.25	-
Rinter Interface reduction factor (R_{int})	0.8	0.8	0.8	-
EA (kN/m2)	-	-	-	2000

3. Methodology Of PLAXIS 2D Calculation

The ultimate bearing capacities for the footing-soil system are determined from the load-displacement curves. The test program primarily consisted of load tests on a model strip footing placed on top of a reinforced or unreinforced sand. Load-settlement curves were obtained for the software results. Since there was no definite failure point observed in the load-settlement curves, the ultimate bearing capacity capacity was determine by the following method. Tangent lines were drawn from the initial and end points of the load-settlement curve and the point of intersection of these tangents was produced back to the y-axis to obtain the ultimate bearing capacity (q_u).

$q_{u(R)}$: the ultimate bearing capacity of eccentrically loaded strip footing on reinforced sand.

$q_{u(UR)}$: the ultimate bearing capacity of centrically loaded strip footing on unreinforced sand.

Another, factor to consider for the efficiency of the reinforcement is the settlement characteristic of the system (S) which obtained at the ultimate bearing capacity conditions for the reinforced and unreinforced soil.

Also, the effective depth zone of the reinforcement (d_e) is the depth beneath the footing base, under which no longer effect of the reinforcement on the bearing capacity is observed. This depth could be calculated as follow:

$$d_e = u + (N-1)\, h \qquad (1)$$

Where:

d_e: the effective depth zone of the reinforcement.
u: the depth between the footing base & the first layer of reinforcement.
N:the number of reinforcement layers.
h: the depth between reinforcement layers.

In PLAXIS code, geogrid are flexible elastic element that represent a grid or sheet of fabric. Geogrid cannot sustain compressive forces. The only property in a geogrid data

set is elastic axial stiffness(EA), interred in units of force per unit width. The axil stiffness, EA, is usually provided by the geogrid manufacturer and can be determined from in which the elongation of the geogrid is plotted against the applied force in a longitudinal direction. The axial stiffness is the ratio

of axial force per unit width and axial strain

$$EA = F/(\Delta l/l) \qquad (2)$$

Where:

Δl/l is the elongation.

l is the length

After the generation of a finite element model, the actual finite element calculations can be executed. Therefore, it is necessary to define which type of calculations is to be performed and which of loading or construction stages are to be activated during the calculations.

3.1 Defining A Calculation Phase

In this study two calculation phases are considered. The first one is the initial phase, which phase number is 0. This line represents the initial situation of the problem as defined in the initial conditions mode of the input program. The initial phase is the starting point for further calculations while, the second phase include the external line load. When the calculations program is started directly after the input of a new problem, a first calculation phase is automatically inserted. In order to simulate the settlement of the footing in this analysis a plastic calculation is required. PLAXIS has a convenient procedure for automatic load stepping, which is called load Advancement. This procedure can be used for most practical applications. Within the plastic calculation, the prescribed displacements are activated to simulate the indentation of the footing. In PLAXIS, these processes can be simulated by means of the staged constriction calculation option. Staged constriction can be used to change material properties, water pressure distribution and to simulate excavations or constructions.

4. PLAXIS OUTPUT

4.1 Deformations

One of the most important outputs of PLAXIS calculation is the displacement. The total displacement are the absolute accumulated displacement (u), combined from the horizontal (x) and vertical (y) displacement components at all nodes at the end of the current calculation step, displayed on plot of the geometry. Similarly, the horizontal displacement and vertical displacement are, respectively, the accumulated horizontal (x) and vertical (y) displacement components at all nodes at the end current calculations step. The output for a geogrid comprises deformations and forces. Tensile forces in geogrid are always positive. Compressive forces are not allowed in these elements.

4.2. Analysis and Plot of the Results

The deep analysis of the results has been carried out to observed the difference between various parameters

Table 4 The ultimate bearing capacity when eccentrically loads acting on the footing with three types of unreinforced soil

Test No.	Soil type	Eccentricity Value (e_l/B)	Ultimate load P(kn)	Settlement (S) $*10^{-3}$ (m)	Ultimate bearing capacity Without geogrids $q_{u(UR)}$ (kn/m^2)
1	Dense	0	315	2.545	334
2		0.05	223	1.892	271.29
3		0.1	178	1.672	251.17
4		0.13	130	1.256	233.61
5		0.15	101	1.123	198.42
1	Medium	0	150	2.051	163.66
2		0.05	99	1.401	116.12
3		0.1	78	1.200	106
4		0.13	64	1.054	103.97
5		0.15	53	0.834	87.70
1	Loose	0	80	2.984	104.13
2		0.05	66	2.809	91.04
3		0.1	50	2.439	84.96
4		0.13	41	1.993	79.92
5		0.15	33	1.469	65.94

Table 5 The ultimate bearing capacity when eccentrcal loads acting on the footing with three types of sands reinforced symmetrically

Test No.	Soil type	Eccentricit Value (e_l/B)	Ultimate load *P(kn)*	Settlement *S *10^{-3} (m)*	Ultimate bearing capacity With symmetrical geogrids $q_{u(R)}$ (kn/m^2)
1	Dense	0	557	5.116	700.65
2		0.05	319	2.870	485.20
3		0.1	250	2.620	435.22
4		0.13	213	2.485	395.22
5		0.15	188	2.325	321.42
1	Medium	0	231	4.337	324.38
2		0.05	156	2.974	221.25
3		0.1	118	2.245	199.34
4		0.13	102	2.068	192.6
5		0.15	79	1.382	151.51
1	Loose	0	122	4.618	187.73
2		0.05	94	3.921	158.22
3		0.1	73	3.786	144.37
4		0.13	61	3.252	132.93
5		0.15	51	2.457	106.76

Table 6 The ultimate bearing capacity when using various number of geogrid layers in dense sand.

Test No.	No. of ge- ogrids Layers (N)	Eccentricity value (e_l/B)	Ultimate load *P(kN)*	Settlement $S *10^{-3}$ *(m)*	Ultimate bearing capacity with geogrids $q_{u(R)}$ *(kn/m²)*
1	1	0.1	208	1.931	292.69
2	2		224	2.486	301.37
3	3		236	2.522	431.46
4	4		250	2.620	435.22
5	5		252	2.629	437.13
1	1	0.15	111	0.998	188.53
2	2		125	1.650	200.11
3	3		138	1.973	239.47
4	4		188	2.325	321.42
5	5		190	2.370	322.8

Table 7 The ultimate bearing capacity of using various lengths of geogrid layer in dense sand.

Test No.	L/B	Eccentricity value (e_l/B)	Settlement $S *10^{-3}$ *(m)*	Ultimate bearing capacity With geogrids $q_{u(R)}$ *(kN/m²)*
1	2	0.1	19.11	286.28
2	3		22.87	361.86
3	4		42.19	398.6
4	5		25.25	435.22
5	6		28.35	435.47
1	2	0.15	11.3	198.12
2	3		13.9	214.17
3	4		15.4	235.11
4	5		17.7	267.25
5	6		17.9	267.62

Table 8 The ultimate bearing capacity of using various lengths of geogrid layer in medium dense sand.

Test No.	L/B	Eccentricity Value (e_l/B)	Settlement $S *10^{-3}$ *(m)*	Ultimate bearing capacity $q_{u(R)}$ *(kN/m²)*
1	2	0.1	16.18	147.27
2	3		20.68	161.31
3	4		21.37	174
4	5		22.45	199.34
5	6		22.7	197.6
1	2	0.15	9.12	100.12
2	3		10.6	109.77
3	4		11.43	118.14
4	5		12.11	127.93
5	6		12.17	128

Table 9 The ultimate bearing capacity when laying the geogrid layers with different eccentricities (e_G/B) with a centrically & eccentrically loaded footing (e_l/B =0, 0.1, & 0.15).

Test No.	(e_G/B)	(e_l/B)	Ultimate load *P(kN)*	Settlement $S *10^{-3}$ *(m)*	Ultimate bearing capacity $q_{u(R)}$ *(kN/m²)*
1	-0.08	0	551	48.37	694.12
2	0.07		555	51.1	698
3	0.08		551	48.37	694.12
4	0.1		556	50.8	699.11
5	0.25		535	50.12	689.81
6	0.42		495	49.82	623.67
1	-0.08	0.1	252	26.03	389.76
2	0.07		255	27.13	452
3	0.08		305	32.86	495.17
4	0.1		297	32.46	489.12
5	0.25		262	27.61	419
6	0.42		240	27.17	400
1	-0.08	0.15	100	12.3	212.14
2	0.07		160	19.9	347.17
3	0.08		183	24.2	387.15
4	0.1		173	23.14	372.43
5	0.25		142	16.17	285.34
6	0.42		119	13.55	277.68

4.2.1The Effect of Load Eccentricity

Six series of tests were carried out on a model strip footing supported on reinforced sand to evaluate the effect of the load eccentricty. While the first three series were carried out on unreinforced sands as illustrated in table (4), the other three series were carried out on four symmetrical layer geogrid-reinforced sand at the same values of (eL/B) ratio of 0.05, 0.1, 0.13, and 0.15 as shown in table (5). The sand were inserted in the analysis with three unit weights representing dense, medium dense, and loose relative densities. These tests were simulated on prototype footing using FEA.

The test results of prototype footing shows that the effect of soil reinforcement on the bearing capacity are greater at lower values of the ratio (eL/B) and greater values of relative density as shown in figure 3. However, the rate of decrease in the ultimate bearing capacity with (eL/B) is significant until the value of eL/B= 0.15 after which the effect becomes much lower. For example, eL/B= 0.1, the gain in the ultimate bearing capacity are 69.93%, 88.06%, and 73.28% for loose, medium dense, and dense sands, respectively. figure. 4 shows the effect of eccentricity on the bearing capacity with various relative densities of sandy soil.

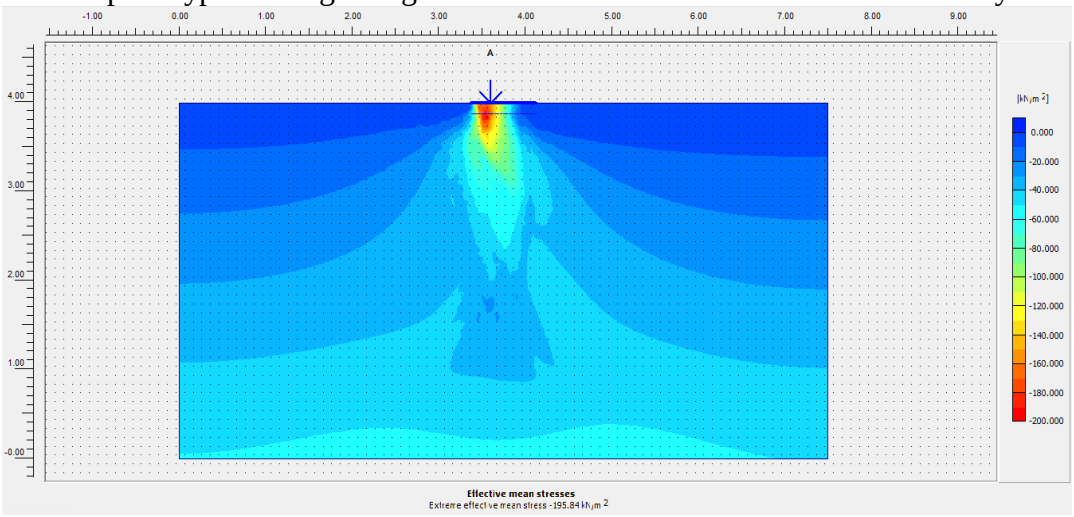

Fig. 3 Stress for unreinforcing soil.

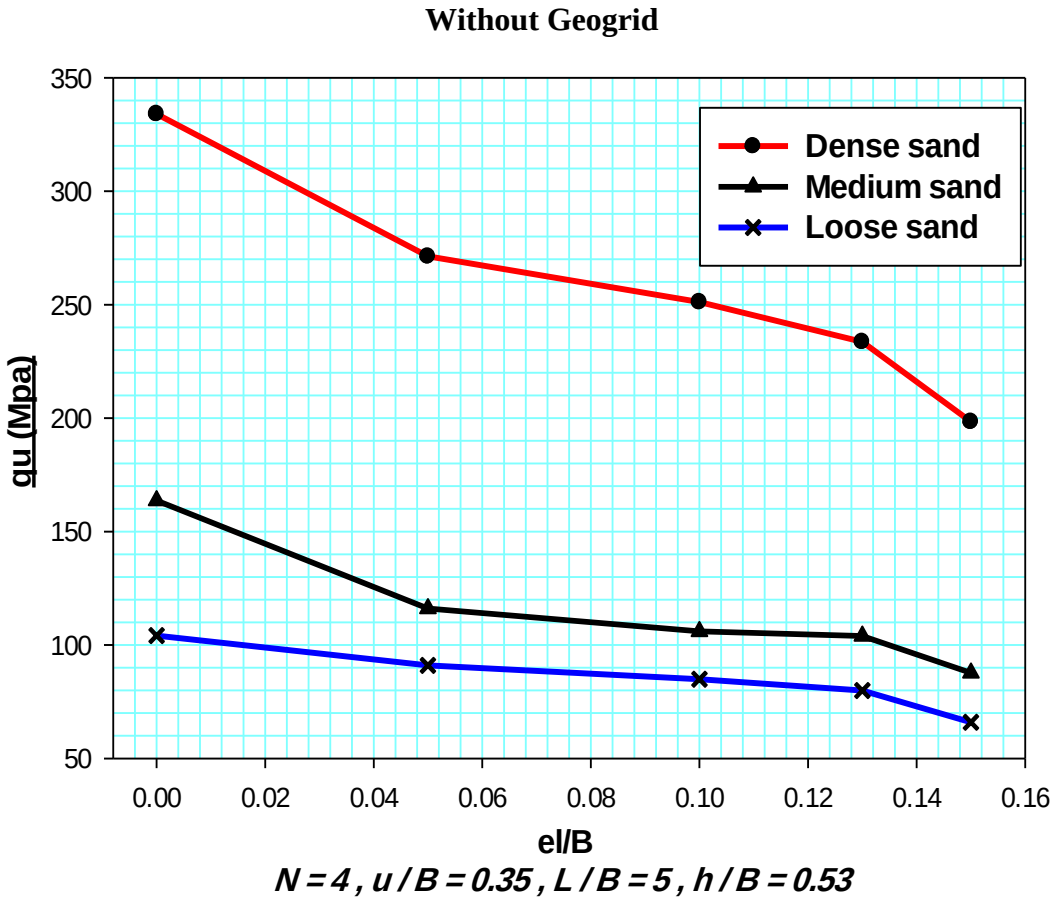

Fig.4 qu VS. el/B for the three type of sandy soil.

With taking into account the optimum value of the following parameters u/B=0.35, h/B=0.53, L/B=5 and N=4, the ultimate bearing capacity significantly improved as shown in figure. (6) in dense sand the increasing rate up to 44.4% between the centric load on the footing and first eccentricity ratios of (el/B=0.05), then the improvement rate become stable in reduction till the end of loading since the reduction rate at the last two eccentricity ratios are almost 23% and the same ternd behavior of the medium and loose sand.

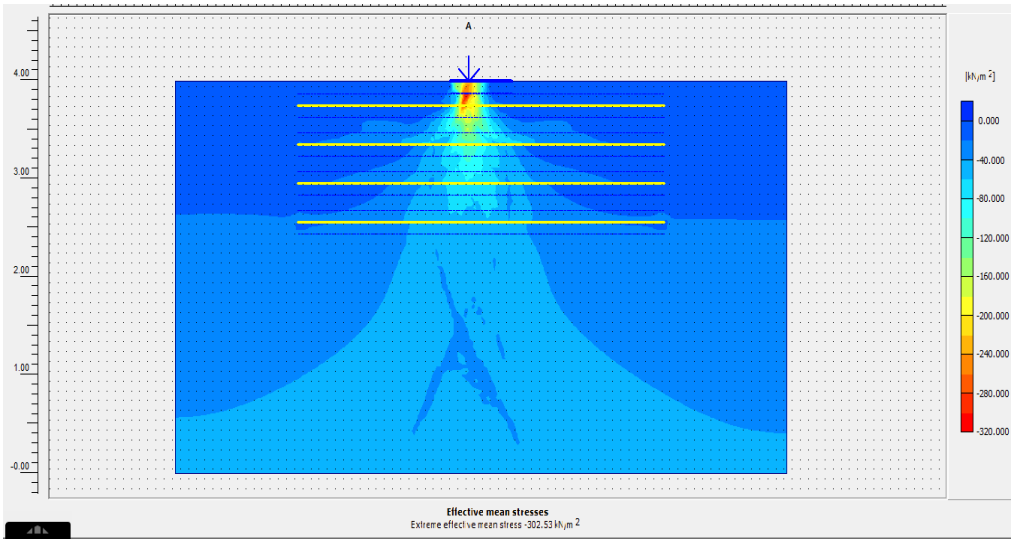

Figure .5 stress for reinforcing soil.

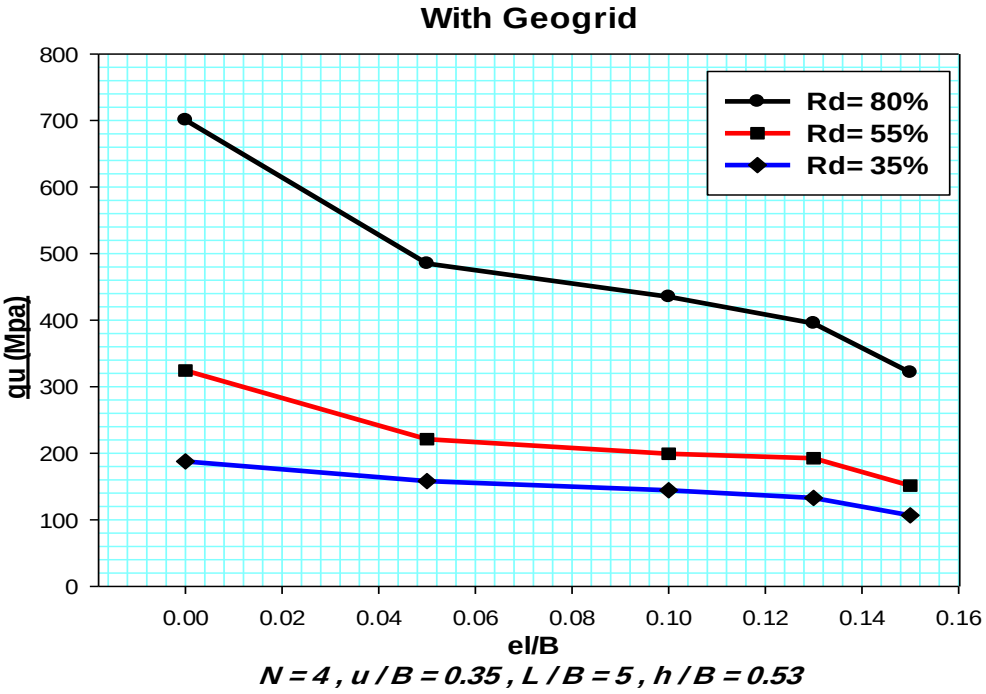

Fig. 6 qu VS. el/B for the three type of reinforced soil.

the following three figures are showing the impact of eccentricity ratio el/B on the load value, the load decreases by increasing the eccentricity and that is clear in the following three figures(7, 8, & 9) and the load value is much improving within laying the geogrid layer, this improvement up to 42.42% in loose sand ,57.5% in medium sand and43.4% in dense sand

.

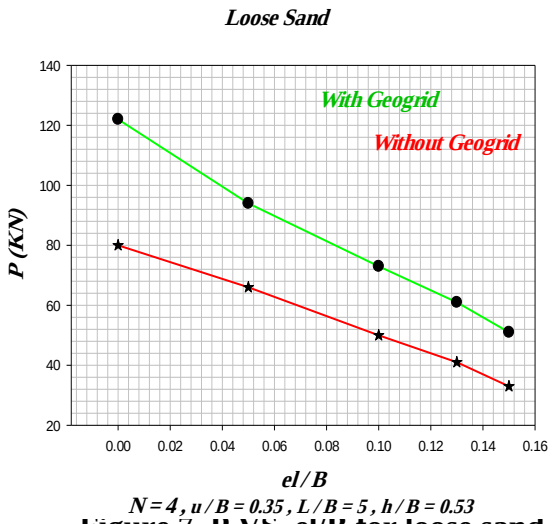

Figure.7 P VS. el/B for loose sand with with and without reinforcing.

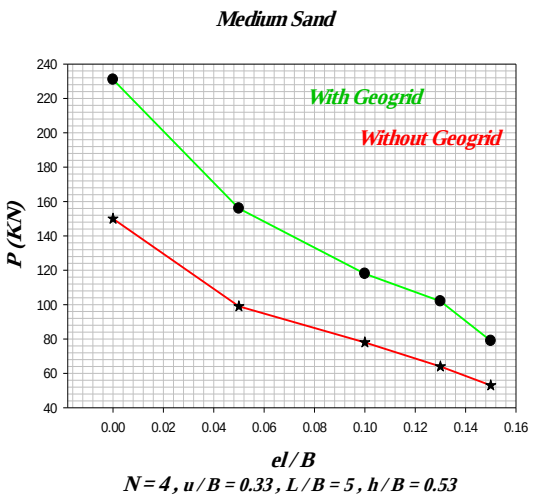

Figure.8 P VS. el/B for medium sand and without reinforcing

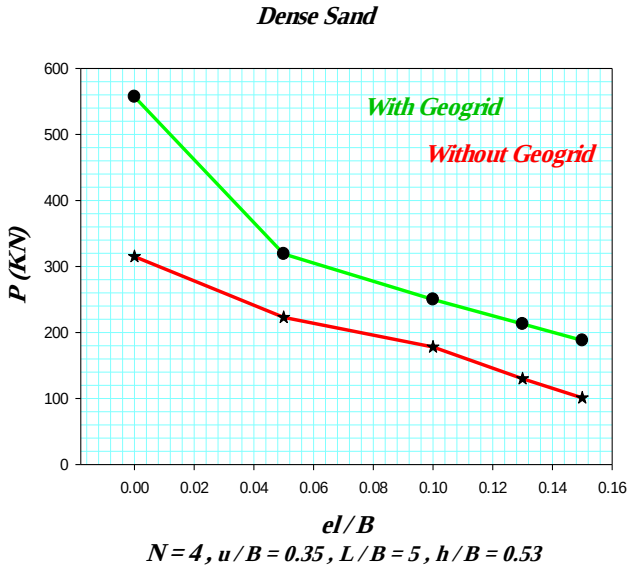

Fig. 9 P VS. el/B for dense sand with and without reinforcing.

4.2.2The Effect of Number of Geogrid Layers

Five tests were carried out with all the variables were kept constant expect the number of layers was variable. Various number of geogrid layers that tested (N) of 1,2,3,4, and 5, were for eL/B=0.1 and eL/B=0.15. The figures (10,11) clearly indicate that the ultimate bearing capacity much improves with the number of geogrid layers for both values of eccentricity (eL/B) the bearing capacity increases with increasing number of geogrid layers until N=4 after which the rate of load improvement becomes much less. It should be mention that the optimum number of geogrid layers is much dependent on the vertical spacing between geogrid layers and

embedment depth of the first layer . This is due to the fact that soil reinforcement is significant when placed in the effective zone under the footing. When el/B = 0.1 as showing in the figure (11) there is a significant increase in the bearing capacity (qu) has been observed up to N= 4, after that there is not significant increase in it. Figure (16) demonstrate that the bearing capacity increase by increasing the geogrid layers up to N=4 , then the curve get stable, so, the optimum number of geogrid layers are (N=4) .

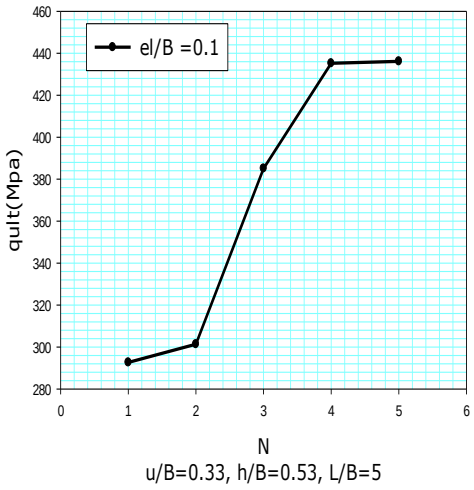

Figure.10 q_{ult} VS. N for dense sand sand at el/B= 0.1.

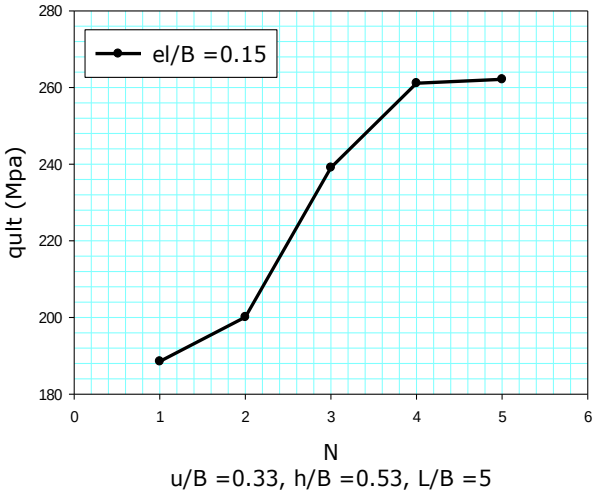

Figure.11 q_{ult} VS. N curve fore dense with el/B = 0.15.

4.2.3. The Effect of Geogrid Layer Length

Twenty numerical models in four series were carried out to determine the adequate length for geogrid layer. The parameters u/B=0.33, h/b=0.53 and L/B=5 were kept constant with varing only the layer length (L/B) of 2, 3, 4, 5, and 6 for the medium dense, dense sands, and load eccentricity of (e_L/B= 0.1 and e_L /B= 0.15). Results of prototype footing are plotted in figures (12,13). It is clear that the (q_u) increases with increasing geogrid layer length. Soil reinforcement placed in dense sand had a greater effect than when it located in medium dense sand for both (e_L/B) ratios. However, this improvement in the ultimate bearing capacity with increasing layer length is significant until a value of (L/B=5) beyond this which further increase in layer length of geogrid does not show significant contribution in improving the ultimate load of the footing. Figures (12,13) show the relationship between the ultimate bearing capacity and (L/B) for different soil densities and (e_L/B), the value of q_{ult} increases as the *(L/B)* ratio increases and significant increase in q_{ult} has been observed upto (L/B=*5)*, after that there is not significant increase in q_u. Based on this improvement in the bearing capacity, L = 5B may be taken as effective length of the geogrid layer. The maximum improvement in the bearing capacity with the optimum length of geogrid layer of tested soil is up to 76 % in dense sand and 85% in medium dense sand,

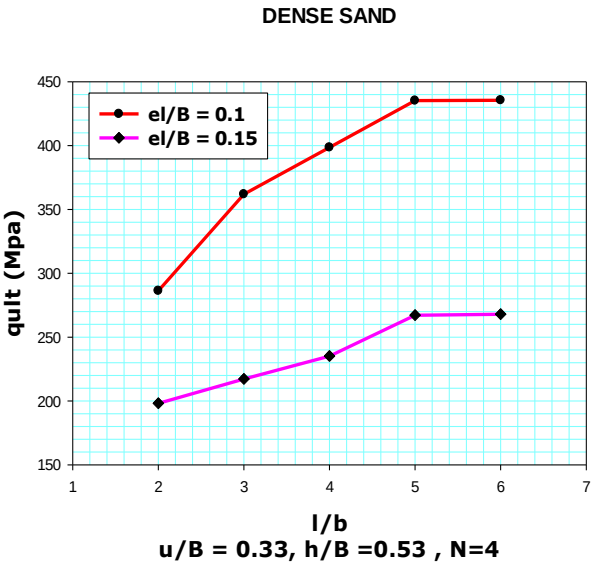

Fig. 12 q_u VS. L/B for dense sand

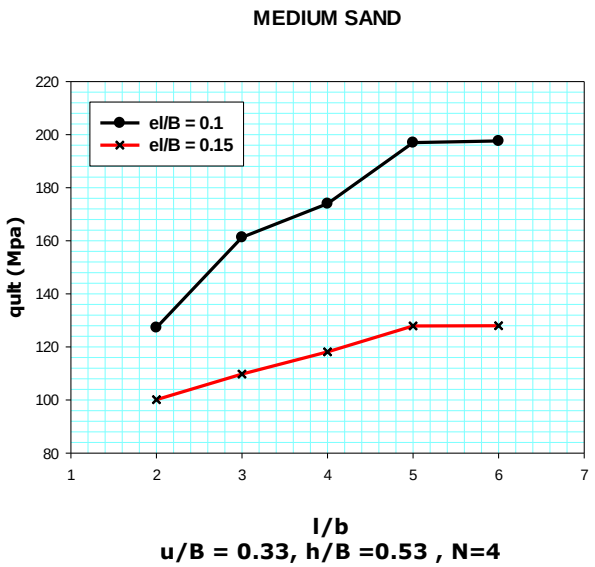

Fig. 13 q_u VS. L/B for medium sand

4.2.4 The Effect of Geogrid Layer Eccentricity

Eighteen numerical models in three series were performed on dense sand with unsymmetrical geogrid layers. Each series was carried out for a specific load eccentricity ratio (e_L /B=0, 0.1, and 0.15) using the same parameters (N=4 and L/B=5) except that the location of geogrid layers relative to the footing width was varied (e_G /B= 0.42, 0.25, 0.1, 0.08, 0.07and -0.08). The variations of q_u that obtained from numerical analysis against (e_G/B) ratio for different (e_L/B) ratio shown in figure14. The figure 14 clearly shows that, the footing response much improved as the ratio (e_G/B) decreases comparing to the situation when the layers were placed almost symmetrical under the footing. The rate of improvement in the ultimate bearing capacity reaches to 13.77% comparing with laying the layers symmetrically under the footing and 97.14 % comparing with the soil without geogrid at the same eccentricity value. The same behavior with e_L/B =0.15 which in the blue color curve, but the improvement rate bigger than the previous one where it up to 45.98 % comparing with symmetrical layer and 127 % with comparing of soil without reinforcing, the value e_G/B = -0.08 was laid to know the impact of making e_G/B value in opposite direction of eccentricity load center and the results showed the same value when the load in the other part of the center and no improvement in bearing capacity. The figure 14 demonstrates that no significant change on q_u improvement when the load is applied in the next part of the center of the footing. It is clearly to notice that the q_{ult} began to increase with increase of geogrid eccentricity up to e_G/B= 0.08 then the curve starts to decline, this behavior is similar in value of el/B =0.1 and e_L/B =0.15. So, the optimum value of (e_G) that given maximum bearing capacity is obtained when the geoagrid is lied with eccentricity equal to 0.08B.

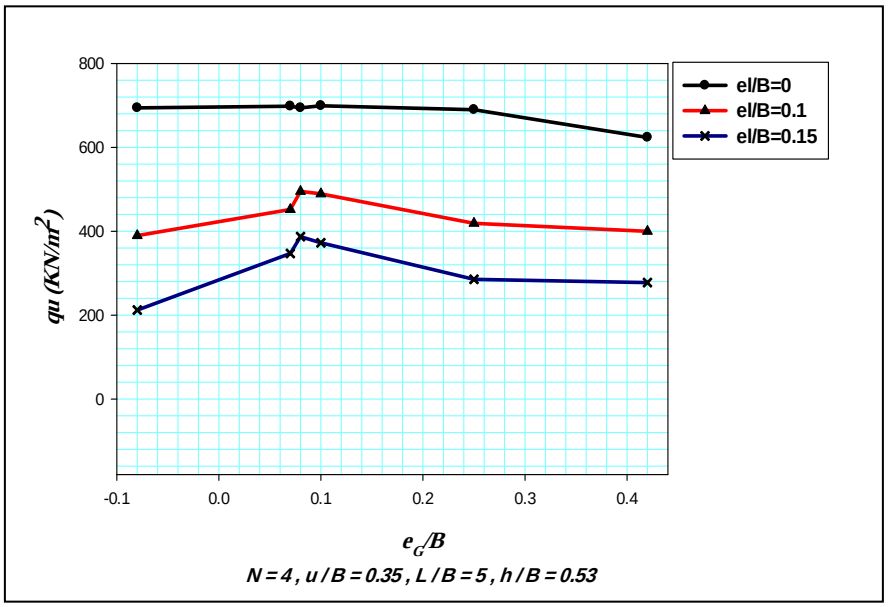

Fig. 14 q_u, VS. e_G/B for dense sand with various eccentricity.

5 CONCLUSION

In this study a brief conclusion is presented as following :

(1The load eccentricity significantly reduces the ultimate bearing capacity of strip footing resting on sand and it significantly affects most of the reinforcement parameters. The gain in the bearing capacity of the model footing are 57.6, 68.3, and 55.6% for loose, medium dense, and dense sands, respectively with unreinforcing sand

(2Soil reinforcement significantly improves the ultimate bearing capacity of an eccentrically loaded strip footing leading to significant decrease in the footing size and the value of eccentricity and therefore better performance and economic design of the footing, this improvement up to 42.42% in loose sand, 57.5% in medium sand and43.4% in dense sand.

(3The effect of soil reinforcement on the qu is greater at lower values of eccentricity and greater relative densities. However, the qu significantly decreases as the ratio eL/B increases until a value of eL /B=0.15.

(4Vertical displacement values at failure decrease with increasing eccentricities in both unreinforced and reinforced test cases.

(5Finally, the inclusion of the geogrid layers with eccentricities under eccentrically loaded strip footing has significant effect on the behavior of the footing. For unsymmetrical layer placement, the incensement in the bearing capacity ratio is13.77% comparing with the laying layers symmetrically, and 97.14 % comparing with soil without geogrid at eL/B= 0.1, and

% 45.98comparing with symmetrical layer and 127 % comparing with soil without reinforcing at el/B =0.15. The qu improves with the increase in number of geogrid layers when sufficient lengths were provided the optimum number of geogrid layers is (N=4). The recommended L/B ratio should be five times of the footing width (L/B=5).

6 REFERENCES

[1] A. RAHMAN AL-SINAIDI & ASHRAF HASSAN ALI. 2015. "Improvement in bearing capacity of soil by geogrid – an experimental approach" IAEG2006 Paper number 240. PP. 1-5.

[2] A. Zhusupbekov & R. Lukpanov & T. Muzdybaeva . 2006 "Bearing capacity of eccentrically loaded strip foundation on geogrid- reinforced sand", L.N. Gumilyov Eurasian National University, Kazakh- stan. PP.861-864.

[3] Ahmed M. A. Nasr, Waseim R. Azzam. 2017."behavior of eccentrically loaded strip footing resting on sand". International Journal of Physical Modelling in Geotechnics, Volume 17 Issue 3, September, 2017, pp. 177-194

[4] E. Badakhshan, & A. Noorzad. 2017."Effect of footing shape and load eccentricity on behavior of geosynthetic reinforced sand bed". Shahid Beheshti University, Tehran, Iran. Geotextiles and Geomembranes, PP. 58-67.

[5] E. Sadoglu et al . 2009"Ultimate loads for eccentrically loaded model shallow strip footings on geotextile-reinforced sand", Department of Civil Engineering, Cumhuriyet University, 58050 Sivas, Turkey. PP.176- 182.

[6] Gaoqiao Wu, Minghua Zhao, Rui Zhang, Guanting Liang 2020. "Ultimate bearing capacity of eccentrically loaded strip footing above voids in rock masses" .Computers and Geotechnics 128,103819

[7] Hamed J., Abdolosein H. & Behrooz M. 2012."Experimental and Numerical Investigation of the Bearing Capacity of adjacent footings on reinforced soil". EJGE, Vol. 17, Band. R.

[8] Jawdat K. Al-Tirkity and Akram H. Al-Taay. 2012. " Bearing Capacity of Eccentrically Loaded Strip Footing on Geogrid Reinforced Sand". Tikrit Journal of Engineering Sciences/Vol.19/No.1 /March, PP.14-22.

[9] Kolay, P. K., Kumar, S.& Tiwari, D. 2013. "Improvement of Bearing Capacity of shallow foundation on geogrid reinforcement silty caly and sand " Journal of construction Eng. Article, ID 293809, PP.1-10.

[10] Mostafa A. EISa. & Ashraf K. N. 2012. " Cyclic settlement behavior of strip footings resting on reinforced layered sand slop". Journal of Advanced research, Vol. 3, PP. 315-324.

[11] Patra, C. R., Das B. M., Bhoi, M. and Shin, E. C. 2006. "Eccentrically Loaded Strip Foundation on Geogrid-Reinforced Sand", Journal of Geotextiles and Geomembranes. 24, PP. 254-259.

[12] Shin, E. C. & Das, B. M. 2000. "Experimental study Bearing Capacity of a strip foundation on Geogrid-reinforced sand". Geosynthetic international, Vol.7, No.1, PP.59-71.

[13] Wajeeh Mohammed, T. P. & IIamparuthi K. 2010. "performance of footing on sand bed with and without Reinforcement". CEG, Anna University Chennai, Mumbai, India